Effect of non-stationary current regimes on the morphology of silver electrodeposits

ALEKSANDAR T. DIMITROV[1]*, PERICA PAUNOVIĆ[1], ORCE POPOVSKI[2], DRAGAN SLAVKOV[1], ŽELJKO KAMBEROVIĆ[3] and SVETOMIR HADŽI JORDANOV[1]

[1]Faculty of Technology and Metallurgy, University "St. Cyril and Methodius", Skopje, [2]Military Academy "Mihajlo Apostolski", Skopje, FYR Macedonia and [3]Faculty of Technology and Metallurgy, University in Belgrade, Serbia

Abstract: This work is concerned with the use of reverse current regimes in order to form small-grained and compact silver deposits during the electro-refining process. Several parameters were varied, *i.e*., *i*) anodic overpotential, *ii*) cathodic *vs*. anodic time ratio and *iii*) duration of the anodic pulse. After optimization of these parameters, phosphate ions were added and the electro-lyte was stirred. The effects of a rise of the anodic overpotential on the grain sizes of the silver deposit and compactness were studied. Prolongation of the anodic time had a similar influence but with a decrease in current efficiency. An increase of the cathodic *vs*. anodic time ratio caused an enlargement of the grains and a decrease in the compactness of the deposit. Optimal morphological characteristics were obtained when PO_4^{3-} were added and the electrolyte was stirred.

Keywords: silver; reverse current; electrorefining; nitrate solution; electrodeposition.

INTRODUCTION

Morphology, which depends on kinetic parameters of the electrodeposition process, overpotential and current density, is considered to be one of the most important features of electrodeposited metals. Traditionally, silver produced by electrorefining from nitrate electrolytes is of dispersed shape (mostly dendritic and spongy).[1] Compact and technically applicable metals are produced by a further smelting/casting procedure.[2]

In order to explain why silver deposits are preferentially dendritic, both electrochemical and crystallographic aspects were considered. Granular deposits of high porosity at lower overpotentials and dendrites at higher ones are the result of the high value of the silver exchange current density (low j/j_0 ratio).[3] On the

other hand, non-compact silver layers are formed due to hindered nucleation. Markov *et al.*[4] showed the existence of a wide nucleation exclusion zone near each nucleus growing on a foreign substrate, and Milchev[5] the same in the case of silver. The generation and growth of nuclei is followed by the formation and growth of the nucleation exclusion zones. As a result, the nucleus surface density is low and hence rough and uneven deposits are formed during further growth.

Normally, direct formation of compact silver deposits is preferable. This leads to a simpler and cheaper electrorefining process as well as a higher level of purification. In previous papers,[5–7] it was shown that the addition of small quantities of phosphate ions, PO_4^{3-}, and stirring of the nitrate electrolyte, created conditions favorable for compact and small-grained silver deposits. This is probably leads to a maximum of the steady-state electrolysis conditions.

Another approach to improve the morphology of silver deposits is the application of reverse current regimes, which results in the dissolution of dendrites and a smoothing of the deposit during the anode pulse at the working electrode,[6] and a decrease of the size of the nucleation exclusion zone;[7] hence, compacter silver deposits are to be expected.

The main goal of this work was to examine how the reverse current regimes affect the morphology of silver deposits. This involved the selection of the appropriate cathodic and anodic overpotential, cathodic *vs.* anodic time ratio and the duration of the anodic pulse. Simultaneously, the effect of stirring and the addition of phosphate ions were also studied.

EXPERIMENTAL

In order to determine the reference state, silver was deposited by direct current electrolysis at –80 mV, as explained elsewhere.[8] The investigation continued with reverse current electrolysis, with variation of several parameters, *i.e.*, *i*) the anodic overpotential η_a was varied between 40–160 mV, *ii*) the cathodic *vs.* anodic pulse duration τ_c:τ_a, was 8:1, 4:1 and 2:1 and *iii*) the duration of the anodic pulse τ_a (2 and 4 s). All variations were investigated both with and without stirring of the electrolyte and/or addition of PO_4^{3-}.

Electrodeposition was performed in an electrochemical cell consisting of Ag wires (0.5 mm) for both the working and reference electrode and an Ag plate with a much higher surface area as the counter electrode. The electrolyte contained 0.50 M $AgNO_3$ and 1.17 M $NaNO_3$, with a further 0.060 M H_3PO_4 added when required. All chemicals were of p.a. quality, and redistilled and deionized water was used. Both stationary and stirred electrolytes (magnetic stirrer, 400 rpm) were tested. The electrochemical cell was connected with an AMEL electrochemical line (Potentiostat/Galvanostat 2053 and programmable generator 568) and a gas-purification line. All experiments were performed at room temperature.

The obtained silver deposits were examined and documented by a scanning electron microscope (SEM), Hitachi 2000 Delta instrument.

RESULTS AND DISCUSSION

Reverse vs. steady-state electrodeposition

In the preliminary stage, the experiments were aimed at demonstrating the differences between the silver deposits produced by d.c. and those by obtained by reverse current electrodeposition at the same cathodic overpotential. The anodic overpotential in the case of the reverse electrodeposition was randomly chosen and further optimized. Determination of the optimal anodic overpotential will be discussed in the following section. A comparison of the morphology is given in Fig. 1. It is obvious that, in both cases, the crystals possessed an FCC-type lattice. The grains were a combination of cube−octahedron, *i.e.*, cubic crystals with modified corners (see Fig. 2). During the steady-state electrodeposition, some other morphological forms developed as well, *e.g.*, twinned grains (A in Fig. 1) and spiral-like crystals (B in Fig. 1). At the edge of the electrode, dendritic growth started (C in Fig. 1). The morphology of the deposit was heterogeneous and non-compact even at the optimal overpotential for d.c. electrodeposition. The opposite, *i.e.*, homogeneity in size and shape, was produced when current reversal was applied (Fig. 1c). The crystal grains were cubic with modified corners and smaller than in the previous case.
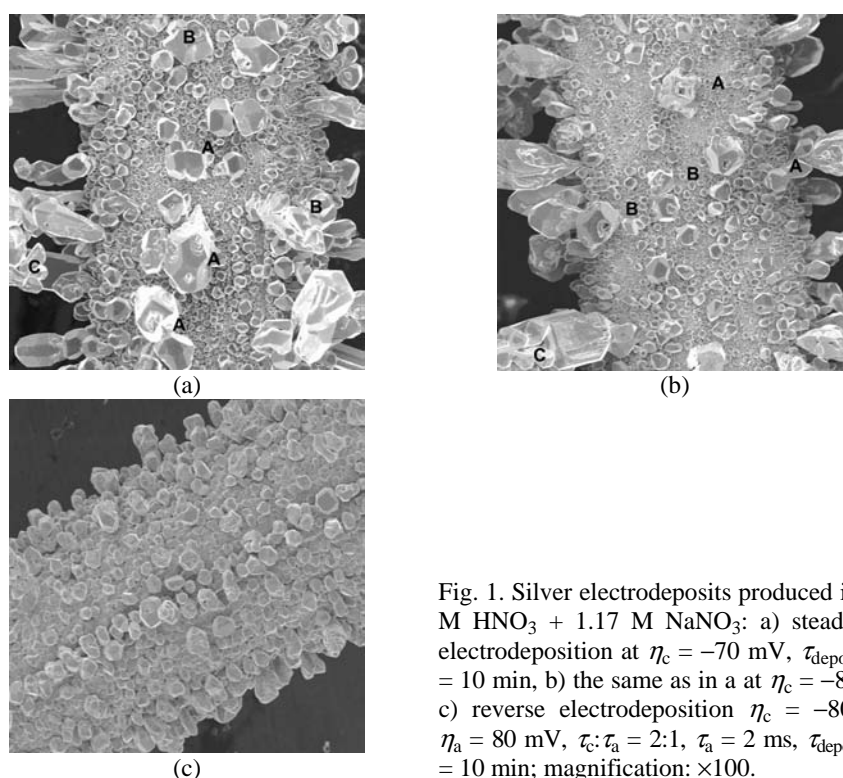

(a)

(b)

(c)

Fig. 1. Silver electrodeposits produced in 0.50 M HNO_3 + 1.17 M $NaNO_3$: a) steady-state electrodeposition at $\eta_c = -70$ mV, $\tau_{deposition} = 10$ min, b) the same as in a at $\eta_c = -80$ mV, c) reverse electrodeposition $\eta_c = -80$ mV, $\eta_a = 80$ mV, τ_c:$\tau_a = 2$:1, $\tau_a = 2$ ms, $\tau_{deposition} = 10$ min; magnification: ×100.
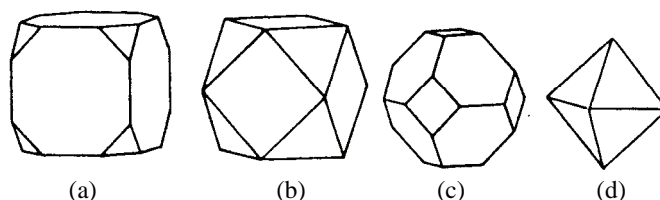
Fig. 2. Transitional shapes from cubic to octahedral: a) initial stage of the modification of the cubic corners, b) and c) different variants of cubic-octahedra, d) octahedral.

During steady-state electrodeposition, the number of nuclei increases, reaching saturation after a certain time (10–100 ms), after which there is no further nuclei formation and only crystal growth occurs. The number of nuclei in the stationary state depends only on the applied overpotential/current density. In the case of the reverse electrodeposition regime, due to the short time of the cathodic pulse, there is no saturation of nuclei formation. After any cathodic pulse, the number of nuclei increases and this contributes to the formation of smaller grains than in the case of steady-state deposition. It should also be mentioned that dissolution of the surface layer occurs during the anodic pulse. This layer contains larger grains and other morphological forms, especially dendrites. As a result of dissolution, a layer with uniform size and shape of grains is formed. The cycle of alternating deposition/dissolution contributes to formation of homogeneous, small-grained and compact deposits.

Variation of η_a and τ_c:τ_a

The first step in the optimization of the parameters of reverse current electrodeposition was an investigation of the influence of the anodic overpotential η_a and the ratio of duration of cathodic *vs*. anodic pulse τ_c:τ_a.

In a previous study,[8] a value of cathodic overpotential of −80 mV was found to be the most suitable, providing the best balance between nucleation and the crystal growth process. Thus, this value was adopted as the value for the cathodic overpotential of the reverse electrodeposition. During the cathodic pulse, deposition of silver occurs as in the case of steady-state electrodeposition but, due to the short duration (shorter than 10 ms), saturation of the nucleation process is not achieved, *i.e.*, the same quantity of metal is dispersed over a larger number of nuclei and, consequently, a small-grained deposit is produced.

On the other hand, during the anodic pulse, several processes occur, such as: *i*) dissolution of all crystals, preferentially at places where the exchange current density j_0 is the highest and *ii*) the splitting off of the crystals weakly bound onto the substrate, especially of larger crystals and dendrites.

The sites of the removed crystals or dendrites are suitable for nucleation in the next cathodic pulse because the nucleation exclusive zones have decreased or completely disappeared. Moreover, they could be also suitable for the growth of neighboring crystals.

The anodic overpotential, η_a, was varied over a wider range of overpotentials, *i.e.*, 40–160 mV. The duration of the anodic pulse τ_a of the reverse cycle is usually shorter than that of the cathodic one τ_c, and in this case it was 2 ms. The ratio of cathodic *vs*. anodic pulse period $\tau_c{:}\tau_a$ was varied as 8:1, 4:1 and 2:1, meaning that τ_c was 16, 8 and 4 ms, respectively.

The change in the morphology of the silver deposits as a function of the variation of the anodic overpotential, η_a, and $\tau_c{:}\tau_a$ is shown in Fig. 3. At lower
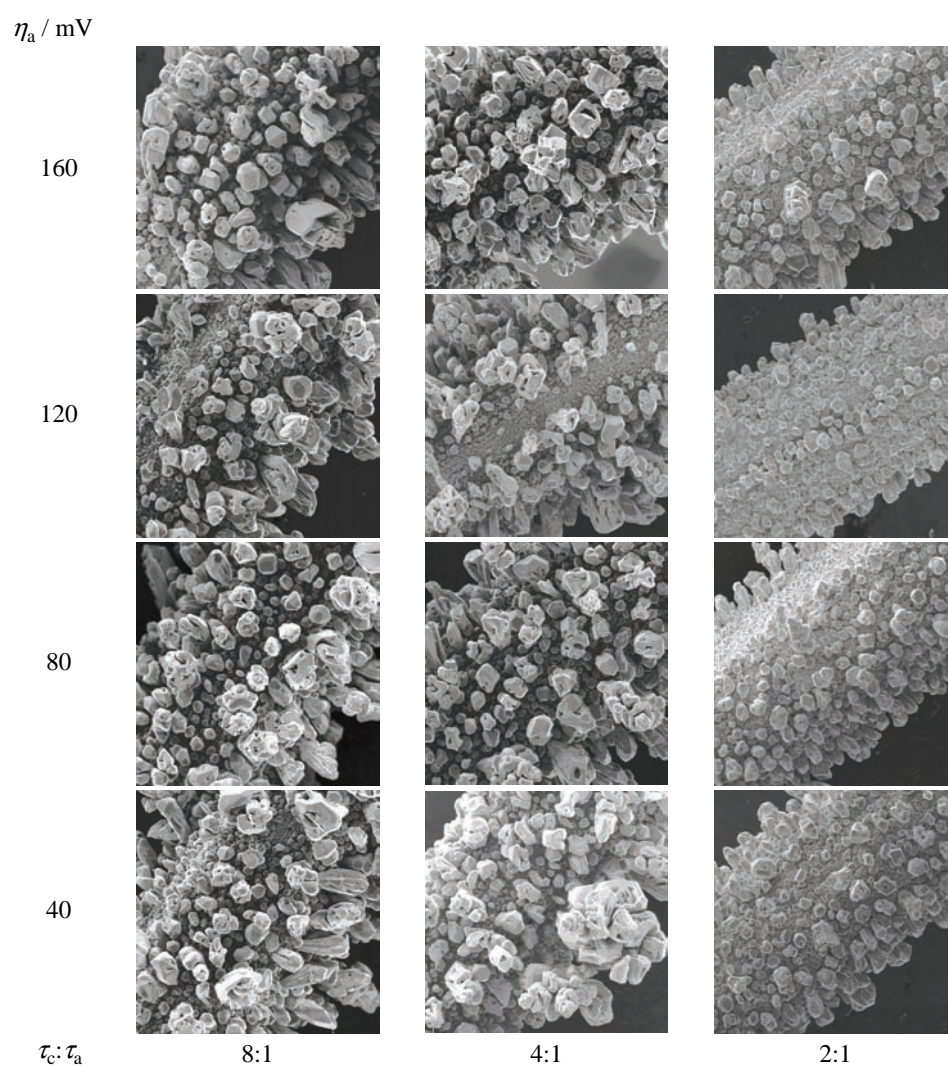
η_a / mV

Fig. 3. Morphological changes of silver electrodeposits as a function of
the anodic overpotential, η_a, and cathodic *vs*. anodic time ratio, $\tau_c{:}\tau_a$;
$\tau_a = 2$ ms, $\tau_{deposition} = 10$ min; magnification: ×100.

anodic overpotential (40 and 60 mV), there was no splitting off or release of the crystals, only a slow dissolution. At higher anodic overpotentials, the tips of the crystals dissolved faster than the side parts. According to their size and shape, it seems that they grew uniformly in all directions. Nevertheless, there was not mutual linking of the crystals. An increase of the anodic overpotential also caused a more intensive dissolution of the larger crystals as well as their splitting and entire release, especially of dendrites. Hence, at an anodic overpotential of 120 mV, the deposits consisted of smaller grains and were more compact than the corresponding ones obtained at lower overpotentials. On further increasing of the anodic overpotential to 160 mV, the grain size and compactness continued to improve. However, considering the lower current efficiency at 160 mV, an anodic overpotential of 120 mV could be regarded as the optimal one.

At the beginning of a cathodic pulse, the nucleation density was high enough for the number of grains to increase and their linkage to occur. It could have been expected that small-grained and compact deposits would continue to improve with further adjustment. However, at the higher ratio of cathodic *vs.* anodic overpotential τ_c:τ_a, saturation of the nucleation could be achieved and crystals grew larger. Even at τ_c:τ_a = 2:1, the obtained deposit was small-grained and compact, but the current efficiency was lower.

Thus, further optimization of the electrolysis parameters was directed towards obtaining small-grained compact deposits with higher current efficiency, *i.e.*, at a higher τ_c:τ_a ratio, *e.g.* 4:1. In order to realize this, the anodic pulse period was varied.

Variation of the anodic pulse period, τ_a

An SEM image of an electrodeposit obtained by reverse electrodeposition with increased duration of the anodic pulse, τ_a = 4 ms, is shown in Fig. 4. Compared with the corresponding deposit obtained under identical conditions but with τ_a = 2 ms (see Fig. 1c), this deposit shows a denser nucleation and close--packed grains of reduced size. Prolongation of the anodic pulse enabled a more intensive dissolution of the larger crystals as well as the release of weaker bound
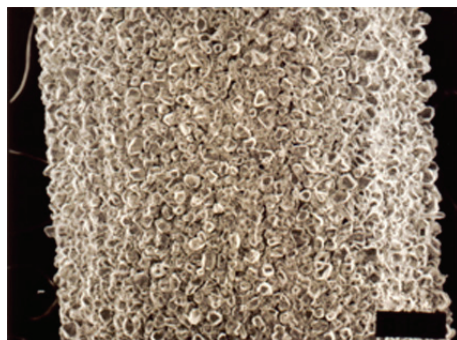

Fig. 4. Silver deposit produced in 0.50 M HNO_3 + 1.17 M $NaNO_3$; η_c = −80 mV; η_a = = 80 mV; τ_c:τ_a = 2:1; τ_a = 4 ms; $\tau_{deposition}$ = = 10 min; magnification: ×100.

crystals from the electrode surface, especially dendrites. Successively repeating the cathodic and anodic pulses resulted in the formation of smaller-grained and more compact deposit. However, the compactness can also be improved with further changes of the electrodeposition conditions, for instance, the addition of PO_4^{3-} and application of stirring to the electrolyte.

Simultaneous action of PO_4^{3-} and stirring of the electrolyte

As mentioned above, formation of compact deposit depends on the j/j_0 ratio. The higher the j/j_0 ratio, the better is the compactness of the deposit. There are several approaches to increase the value of j/j_0, either through increasing the current density, or decreasing the exchange current density, j_0. Further attempts in this study to improve the morphological characteristics of the silver deposits were to include PO_4^{3-} and to stir the electrolyte.

The presence of PO_4^{3-} affects both an increase in the number of active centers and the stimulation of 2D crystal growth. This is a result of lower exchange current density. The values of the exchange current density in nitrate solution with and without PO_4^{3-}, measured by impedance spectroscopy, were 5.0 and 26 mA cm^{-2}, respectively.[6] The polarization curves of the electrodeposition of silver from a solution with and without PO_4^{3-} are shown in Fig. 5. At the potential interval of the formation of polycrystalline deposits, near −80 mV, the current densities were almost the same. Hence, the j/j_0 ratio was more than 5 times higher in the presence of PO_4^{3-} than in their absence. In this case, the nucleation rate increases considerably, while the radius of the nucleation exclusion zones decrease. The large difference in the j_0 values can be attributed to the formation of adsorbed intermediate complexes of Ag$^+$ and PO_4^{3-}, according to the following mechanism:[6,8]
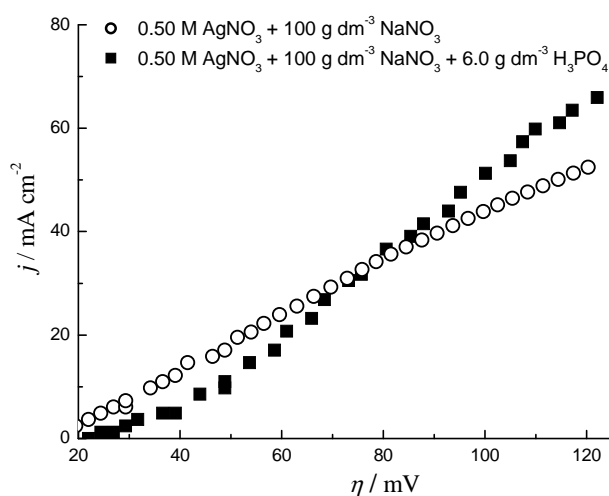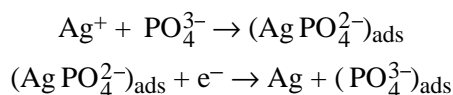

Fig. 5. Polarization curves for a silver electrode in electrolytes with and without PO_4^{3-}.

$$Ag^+ + PO_4^{3-} \rightarrow (Ag\,PO_4^{2-})_{ads}$$

$$(Ag\,PO_4^{2-})_{ads} + e^- \rightarrow Ag + (PO_4^{3-})_{ads}$$

Electrocrystallization processes controlled by incorporation of adatoms suggest two-dimensional (2D) growth. As can be seen from Fig. 6a and 6b, the formed grains had a plate-like shape. As PO_4^{3-} favor the generation of a larger numbers of nuclei and almost eliminate nucleation exclusive zones, the produced deposit was more compact than in the previous cases. Furthermore, if electrolyte stirring is applied, the processes intensify and the deposits were even more compact with smaller grains (Fig. 6c and 6d). The plates were very closely packed and mutually intertwined, thus whisker-like shapes can be observed.
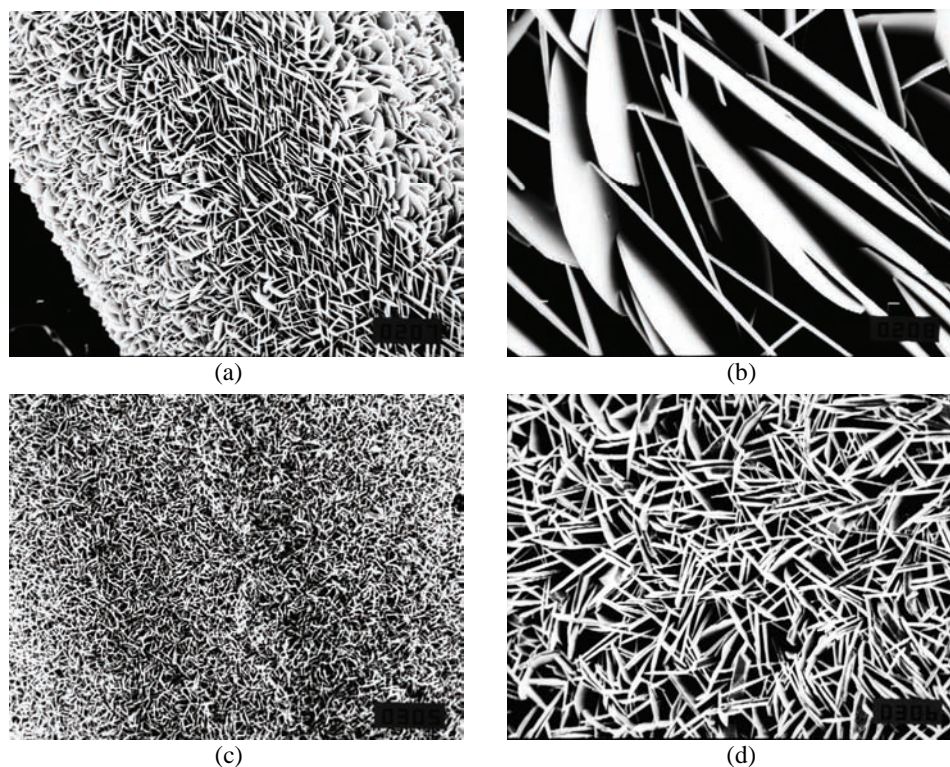

(a)

(b)

(c)

(d)

Fig. 6. Silver electrodeposits produced by reverse electrodeposition in 0.50 M HNO$_3$ + 1.17 M NaNO$_3$ + 0.060 M PO$_4^{3-}$ at $\eta_c = -80$ mV, $\eta_a = 120$ mV, τ_c:$\tau_a = 4$:1, $\tau_a = 4$ ms, $\tau_{deposition} = 10$ min; a) no stirring, magnification: ×100, b) the same as in a), magnification: ×1000, c) stirring 400 rpm, magnification: ×100, d) the same as in c), magnification: ×1000.

Changing the hydrodynamic regime is another approach to increase the j/j_0 ratio. Stirring the electrolyte also lowers diffusion limitations during electrocrystallization. It lowers the concentration gradient that provides a continuous supply

of Ag^+ to the cathode surface. The thickness of the diffusion layer, δ, is also smaller, which means the limiting current density increases. This contributes to an increase in the j/j_0 ratio.

In the case of the simultaneous addition of PO_4^{3-} and stirring of the electrolyte, the j/j_0 ratio increases as a result of both an increase in j due to the stirring of the electrolyte and decrease of j_0 due to introduction of PO_4^{3-}. This enables the formation of compact and small-grained deposits even under conditions when previously this was impossible possible. Figure 7 shows that a fine compact deposit can be obtained at the lower anodic overpotential, 80 mV, and the higher ratio of the duration of the cathodic *vs.* anodic pulse, $\tau_c:\tau_a = 4:1$. This contributes to an improved quality of the deposits and the current efficiency of the electrodeposition process.
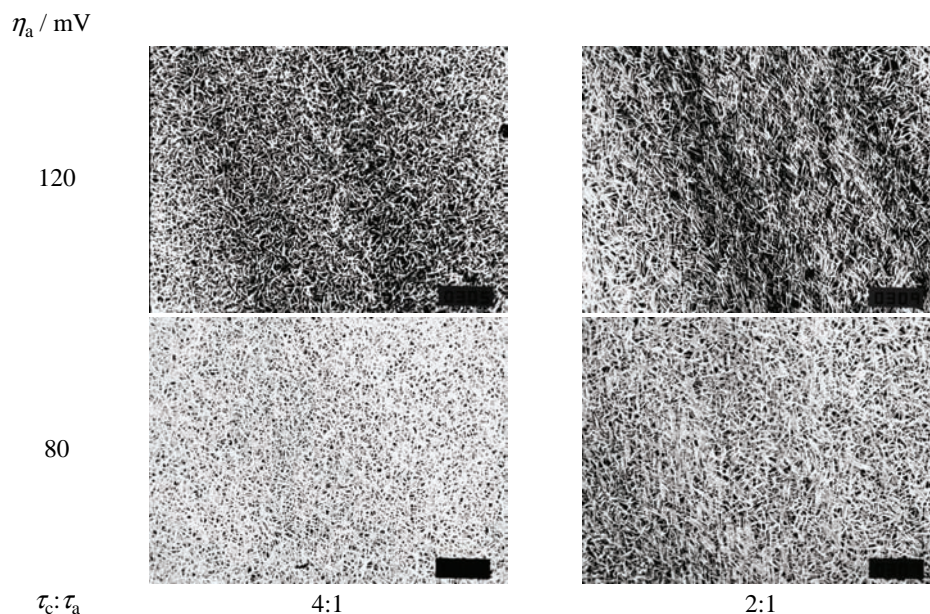

Fig. 7. Morphological changes of silver electrodeposits as a function of anodic overpotential, η_a, and cathodic *vs.* anodic time ratio, $\tau_c:\tau_a$, applying stirring of 400 rpm to the electrolyte; $\tau_a = 4$ ms, $\tau_{deposition} = 10$ min; magnification: ×100.

CONCLUSIONS

The investigations in this study were motivated by the idea to obtain small-grained and compact silver deposits by electrodeposition under electrorefining conditions. After varying several parameters such as anodic overpotential, anodic pulse period, cathodic *vs.* anodic time ratio in stirred and non-stirred electrolyte both with and without the addition of PO_4^{3-}, the following conclusions can be reached:

1) Increasing the anodic overpotential resulted in the formation of smaller grains and increased the compactness of the deposit. An optimal overpotential could be considered 120 mV, because further increasing the overpotential considerably decreased the current efficiency of the electrodeposition process.

2) Increasing the cathodic *vs*. anodic time ratio, $\tau_c:\tau_a$, led to the formation of a rough deposit with larger grains. At $\tau_c:\tau_a = 2:1$, the deposit obtained was compact with smaller grains, but in this case the current efficiency was very low.

3) Prolongation of the anodic pulse had a similar influence on the morphology as the anodic potential, *i.e*., it enabled the formation of a more compact and small-grained deposit. In this case, an appropriate morphology can be obtained at higher cathodic *vs*. anodic time ratios.

4) The addition of PO_4^{3-} and stirring the electrolyte enabled the formation of deposits with the best morphological characteristics at a higher current efficiency.

Reverse current regimes in combination with PO_4^{3-} and stirring of the electrolyte during electrorefining are suitable ways of encouraging the formation of refined and compact silver deposits and they are technically applicable.

И З В О Д

ЕФЕКАТ НЕСТАЦИОНАРНИХ СТРУЈНИХ РЕЖИМА
НА МОРФОЛОГИЈУ ТАЛОГА СРЕБРА

ALEKSANDAR T. DIMITROV[1], PERICA PAUNOVIĆ[1], ORCE POPOVSKI[2], DRAGAN SLAVKOV[1], ЖЕЉКО КАМБЕРОВИЋ[3] и SVETOMIR HADŽI JORDANOV[1]

[1]Faculty of Technology and Metallurgy, University "St. Cyril and Methodius", Skopje,
[2]Military Academy "Mihajlo Apostolski", Skopje, FYROM и [3]Технолошко−меѿалуршки факулѿеѿ,
Универзиѿеѿ у Беоѝраду, Беоѝрад

Рад се бави коришћењем реверсних струјних режима за добијање ситнозрних и компактних талога сребра у процесу електрохемијске рафинације. Варирано је неколико параметара: а) анодна пренапетост, б) однос времена трајања катодног и анодног пулса и ц) трајање анодног пулса. Након оптимизације ових параметара, у електролит су додати фосфатни јони и примењено је мешање електролита. Испитиван је утицај анодне пренапетости на величину зрна талога сребра и на његову компактност. Продужење трајања анодног пулса показало је сличан ефекат, али уз смањење искоришћења струје. Повећање односа времена трајања катодног и анодног пулса довело је до повећања зрна и смањења компактности талога. Оптимална морфологија талога је добијена након додатка PO_4^{3-} и уз мешање електролита.

(Примљено 19. септембра, ревидирано 30. октобра 2008)

REFERENCES

1. A. M. Mosher, *Trans. Am. Inst. Mining. Eng.* **106** (1933) 427
2. C. W. Clark, A. A. Heimrod, *Trans. Electrochem. Soc.* **61** (1932) 77
3. H. Gerischer, *Z. Electrochem.* **62** (1958) 256

4. I. Markov, A. Boynov, S. Toshev, *Electrochim. Acta* **18** (1973) 377
5. A. T. Dimitrov, S. Hadži Jordanov, K. I. Popov, M. G. Pavlović, V. Radmilović, *J. Appl. Electrochem.* **28** (1998) 791
6. K. I. Popov, E. R. Stojilković, V. Radmilović, M. G. Pavlović, *Powder Technol.* **93** (1997) 55
7. N. D. Nikolić, E. R. Stojilković, K. I. Popov, M. G. Pavlović, *J. Serb. Chem. Soc.* **63** (1998) 877
8. A. T. Dimitrov, *PhD Thesis*, University "Sts. Cyril and Methodius", Skopje, 1997 (in Macedonian).